Biointerface Research in Applied Chemistry
Open-Access Journal (ISSN: 2069-5837)

Article
Volume 13, Issue 3, 2023, 284
https://doi.org/10.33263/BRIAC133.284

Flow and Heat Transfer Analysis of a Thin Film Ferromagnetic Liquid over an Unsteady Stretching Sheet

Bhashu Azghar Pasha [1], Mahesha Narayana [2], Ganeshappa Sowmya [1,*], Venkatesh Ramachandramurthy [3]

[1] Department of Mathematics, M S Ramaiah Institute of Technology, Bengaluru – 560 054, Karnataka, India; azpa999@gmail.com (B.A.P.); sowmyag@msrit.edu (G.S.);
[2] Department of Mathematics, The University of the West Indies, Kingston 7, St. Andrew, Jamaica; narayanamahesha@gmail.com (M.N.);
[3] Department of Basic Sciences, R. R. Institute of Technology, Bengaluru, Karnataka, India; ramachandramoorthyv@gmail.com (V.R.);
* Correspondence: sowmyag@msrit.edu (G.S.);

Scopus Author ID 57210621521
Received: 31.03.2022; Accepted: 6.05.2022; Published: 10.07.2022

Abstract: A two-dimensional, unsteady flow of a thin layer of ferromagnetic liquid over a stretching sheet is considered. The flow is exposed to an external magnetic field in the direction of the stretching sheet. The boundary layer equations with the associated boundary conditions are transformed into ODEs using suitable similarity transformations. The resultant system of ODEs is numerically solved using the shooting technique by appropriately guessing the initial values and then correcting them by the Newton-Raphson scheme. The effects of the dimensionless parameters on the flow and heat exchange characteristics are graphically analyzed. It is found that the thickness of the film reduces with magnetization and unsteadiness parameters.

Keywords: liquid film; ferrofluid; stretching sheet; unsteady; magnetization parameter.

Nomenclature: *b*-stretching rate; C_{vh}-specific heat at fixed volume and magnetic field; *H*-external magnetic field; *h*-film thickness; K_0-pyromagnetic coefficient; K^*-magnetization parameter; *k*-thermal conductivity; M-magnetization field; Pr-Prandtl number; S-non-dimensional unsteadiness parameter; *T*-Temperature; T_{ref} -reference temperature; T_s-surface temperature; *t*-Time; *u*-horizontal velocity component; *v*-vertical velocity component; *x*-horizontal coordinate; *y*-vertical coordinate; α-constant; μ-dynamic viscosity; β-dimensionless film thickness; θ-dimensionless temperature; ρ-density; ν-kinematic viscosity; μ_0-magnetic permeability; ψ-stream function.

1. Introduction

Analysis of flow and heat transfer in the liquid film is of immense interest among researchers because of its wide range of applications in industries such as the design of heat exchangers, polymer extrusion processes, process and manufacturing industries, metal casting, steel industries, chemical processing, coating process and so on. Most flow problems relevant to the polymer extrusion process are induced by the stretching motion of a flat elastic sheet. The knowledge of momentum and heat transport in such a process is crucial as the way the sheet is stretched and/or cooled decides the properties of the final product. Proper choice of the coolant is decisive because it affects the cooling rate and spoils the desired quality and characteristics of the end product. Because of such applications, Crane [1] was the first to study the stretching sheet problem in which the velocity was assumed to vary a linear function of the distance from the slit. The exact solution of the Crane problem formally valid for all Reynolds numbers was obtained by Andersson [2] and the pressure distribution, which usually can not be extracted using classical boundary layer theory. Extensive studies on the stretching sheet problem can be found in the literature under various fluid dynamic situations involving various types of cooling liquids (see, Siddheswar and Mahabaleshwar [3], Abel and Mahesha [4], Mahabaleshwar *et al*. [5] and references therein). The Crane problem involves an infinite fluid domain over the sheet. The flow over a stretching sheet with finite fluid domain has attracted many researchers due to its practical applicability in coating processes. Wang [6] was the first to use similarity transformations to solve the governing equations arising in the liquid film over an unsteady stretching sheet that was Newtonian.

However, fluids such as molten plastics and polymers are non-Newtonian and used extensively in the manufacturing industry. The analysis of heat and flow of a thin liquid film is significant in the design and understanding of various chemical processing equipment and heat exchangers. Andersson *et al*. [7] demonstrated the non-Newtonian behavior of thin-film flow of power-law liquid over a time-dependent stretching surface. Andersson *et al*. [8] developed a similar solution for the temperature field to study heat transfer in the flow of liquid film past an unsteady stretching sheet. The effect of thermocapillary was analyzed by Dandapat *et al*. [9], and it was shown that liquid film is pulled in the direction of the stretching sheet due to thermocapillary forces. Dantapat *et al*. [10] showed that the non-uniform distribution of film thickness becomes uniform as the time elapses. Dandapat *et al*. [11] used the perturbation technique to solve the governing equations assuming initial film thickness to be uniform and exhibiting the film's thickness's dependency on the impulsive rate of stretching. Wang [12] used the homotopy analysis method to get the analytical solution for the liquid film flow past an unsteady stretching surface. Chen [13] investigated the viscous dissipation effect on the flow of non-Newtonian liquid film across an unsteady stretching surface. The magnetic field effect, along with viscous dissipation, was analyzed by Abel *et al*. [14] and Santra *et al*. [15] investigated the impact of thermocapillary on the thickness of the film in the flow past a heated stretching surface. Noor *et al*. [16] utilized the homotopy analysis method to examine the influence of liquid thin film on the unsteady stretching sheet in the presence of a magnetic effect. Dandapat *et al*. [17] have studied the impact of thermocapillary in the quicker thinning of the film thickness despite the existence of a magnetic field. Maity [18] observed the thinning of film thickness when the sheet was heated, corresponding to the increasing values of the parameter associated with thermocapillary and the opposite situation when the sheet was cooled. Dandapat *et al*. [19] showed that in comparison with the Newtonian liquid, the thinning of the film is quicker for bi-viscosity liquid. Dandapat *et al*. [20] developed a mathematical model for the flow of a thin double-layer film across a stretching sheet. This work was focused on the film thinning process, and asymptotic solutions were presented for small Reynolds numbers. Recently, Krishnan *et al*. [21] analyzed the impact of porosity, radiative heat flux, applied magnetic field, and thermocapillarity on the flow of thin-film Casson liquid over a stretching sheet. The film thickness was shown to be an increasing function of the thermocapillary number. Some of the recent works based on heat and mass transfer and stretching sheets can be found in [22-34].

There are other industrially important liquids, such as ferrofluids, whose dynamics can be controlled by the external magnetic field, which will assist in achieving desired cooling rate. Because of these properties, ferrofluids have a wide range of applications in magnetic sealing, electronic packaging, computers, solar cells, bioengineering, aerospace, medicine, etc. A ferrofluid can be drawn along the lines of a magnetic field, leading to the development of the pinnacles and valleys due to its nature of getting magnetized strongly and easily in the magnetic field. Nonetheless, surface tension and gravity prevent the expansion of the ferrofluid. Ferrofluids comprise nano-sized particles that become magnetized in a magnetic field. These particles are placed in a carrier liquid (such as water or kerosene) and are covered with a surfactant to keep them from clumping with each other in the liquid. Thermal conductivity is very high in ferrofluids, and they lose their magnetism when heated. The magnetic properties of ferrofluids vanish when they are heated to a sufficiently high temperature called the Curie temperature. Rosensweig [35] studied ferrofluids extensively and documented the findings in the form of a book that covers all the areas of magnetic fluid research, such as synthesis and properties of ferrofluids, theory of ferrohydrodynamics, experimental hydrodynamics in ferrofluids and the description of different applications. This book also presents examples of flow control and magnetic drive, surface and transport instabilities, observations on the induced field, and changes in ferrofluid properties.

Influenced by the industrial applications of ferrofluids, Andersson and Valnes [36] examined the fluid flow on a stretching sheet in the presence of a magnetic dipole, emphasizing the impact of magnetic-thermomechanical interaction on heat transfer and skin friction at the stretching surface. Abel *et al*. [37] discussed the hydromagnetic flow of a micropolar liquid over a stretching sheet. The impact of the magnetic field caused by magnetic dipole on the movement of shear-driven micropolar-ferromagnetic liquid due to a stretching sheet was analyzed by Narayana *et al*. [38]. Majeed *et al*. [39] observed the fluid retardation due to magneto-thermomechanical interaction in the flow of ferromagnetic fluid through a transitional stretching surface due to magnetic dipole. Reddy *et al*. [40] drew attention to the radiating ferrofluid flow due to the slendering stretching surface by considering frictional heating caused by the applied magnetic field. Jalili *et al*. [41] provided solutions using semi-analytical techniques to get the essential properties of the ferrofluid flow. Bhandari and Hussain [42] demonstrated the influence of magnetization and rotational viscosity on ferrohydrodynamic nanofluid flow past a stretching sheet. Some significant recent works based on the phenomenon of ferrofluids can be seen in [43-48].

Studies above on ferrohydrodynamics over a stretching sheet concern the infinite fluid domain. The investigation of ferrofluid flow and heat transfer characteristics of liquid film (finite fluid domain) passed an unsteady stretching surface with an aligned magnetic field has not been explored much in the literature. In the present study, the modeling and computational aspects of -dependent thin film flow of ferromagnetic liquid past a stretching sheet have been discussed numerically by shooting technique.

2. Materials and Methods

2.1. Mathematical formulation.

A two-dimensional, incompressible, unsteady flow of a ferromagnetic liquid film of thickness $h(t)$ caused by the stretching of the horizontal sheet, whose one end is fixed at origin, is shown in Figure 1. The film thickness $h(t)$ is assumed to be uniform and time-dependent.

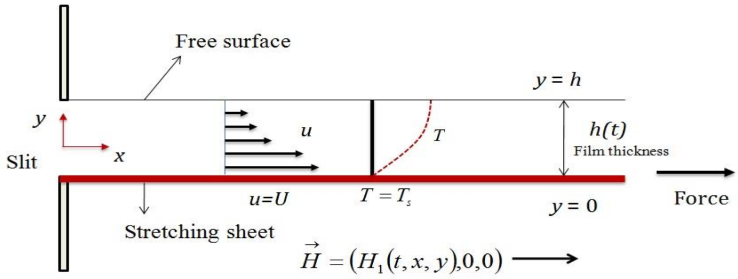

Figure 1. Flow pattern.

The elastic sheet is stretched along the positive x-direction with surface velocity $U(x,t) = bx/(1-\alpha t)$, where $b/(1-\alpha t)$ is the effective rate of stretching which increases with time. Here b and α are positive constants with a dimension per time (Wang [6]). An external magnetic field, $\vec{H} = (H_1(t,x,y),\ 0,0)$ is applied along the direction of the stretching sheet. The temperature T_s at the stretching sheet, $y = 0$ is taken as (see Andersson *et al*. [8])

$$T_s = T_c - \left\{\frac{bx^2}{2\nu(1-\alpha t)^{3/2}}\right\} T_{\text{ref}}, \tag{1}$$

where, T_{ref} and T_c are the reference and Curie temperature, respectively, such that $0 \leq T_{\text{ref}} \leq T_c$.

The following assumptions were made while deriving the governing equations of flow

- The temperature is maintained below the Curie temperature T_c as the magnetic properties of the ferrofluid vanish beyond T_c.
- The thermal conductivity, heat capacity, and viscosity are constants
- Heating due to magnetostriction is negligible
- Displacement currents are neglected
- The viscous dissipation effect is negligible.
- The magnetization vector $\vec{M} = (M_1(t,x,y),0,0)$ is directed along the x-axis.
- The magnetization can be altered by varying the temperature, whereas the effect of viscosity and surface tensions on $\vec{M}$ are negligible.

The governing equations of the flow can be written in the following form:

$$\nabla \cdot \vec{q} = 0, \tag{2}$$

$$\rho\left[\frac{\partial \vec{q}}{\partial t} + (\vec{q}\cdot\nabla)\vec{q}\right] = \mu\nabla^2\vec{q} + \mu_0(\vec{M}\cdot\nabla)\vec{H}, \tag{3}$$

$$\rho C_{vh}\left[\frac{\partial \vec{T}}{\partial t} + (\vec{q}\cdot\nabla)T\right] = k\nabla^2 T \tag{4}$$

Here $\vec{q}$ is the velocity vector, ρ represents the density of the fluid, μ is dynamic viscosity, μ_0 is the magnetic permeability of the free space, k is the thermal conductivity of the ferrofluid, T represents temperature and C_{vh} is the specific heat at fixed volume and magnetic field.

Maxwell's equations for non-conducting fluids are given by

$$\nabla.\vec{B} = 0\,, \tag{5}$$

$$\nabla \times \vec{H} = 0\,, \tag{6}$$

$$\vec{B} = \mu_0\left(\vec{H} + \vec{M}\right). \tag{7}$$

From equations (5)-(7), we get

$$\frac{\partial H_1}{\partial x} = -\frac{\partial M_1}{\partial x}, \tag{8}$$

Incorporating the above information along with the assumptions made, the governing equations (2)-(4) take the following form

$$\frac{\partial u}{\partial x}+\frac{\partial u}{\partial y}=0\,, \tag{9}$$

$$\frac{\partial u}{\partial t}+u\frac{\partial u}{\partial x}+v\frac{\partial u}{\partial y}=\nu\frac{\partial^2 u}{\partial y^2}-\frac{\mu_0}{\rho}M_1\frac{\partial M_1}{\partial x}\,, \tag{10}$$

$$\frac{\partial T}{\partial t}+u\frac{\partial T}{\partial x}+v\frac{\partial T}{\partial y}=\frac{k}{\rho C_{vh}}\frac{\partial^2 T}{\partial y^2}\,, \tag{11}$$

Here, u and v are the components of velocity. The boundary conditions associated with the above system of equations are given below:

$$u=U, v=0, T=T_s \text{ at } y=0\,, \tag{12}$$

$$\frac{\partial u}{\partial y}=\frac{\partial T}{\partial y}=0 \text{ at } y=h\,, \tag{13}$$

$$v=\frac{dh}{dt} \text{ at } y=h. \tag{14}$$

The governing equations are converted to a system of ODE's using the following similarity transformation.

$$f(\eta)=\frac{\psi(t,x,y)}{\left(\frac{b\nu}{1-\alpha t}\right)^{\frac{1}{2}}x},\qquad \theta(\eta)=\frac{T_c-T(t,x,y)}{T_{\text{ref}}\left\{\frac{bx^2}{2\nu(1-\alpha t)^{\frac{3}{2}}}\right\}},\quad \eta=\left\{\frac{b}{\nu(1-\alpha t)}\right\}^{1/2}y. \tag{15}$$

Here, $\nu=\frac{\mu}{\rho}$ is the kinematic viscosity. The component M_1 of magnetization, parameter is taken suitably for similarity as given below (see Andersson and Valnes [36])

$$M_1=K_0x^{-1}(1-\alpha t)^{1/2}(T_c-T), \tag{16}$$

where, K_0 is the pyromagnetic coefficient.

The continuity equation is satisfied obviously with the choice of stream function $\psi(t,x,y)$, such that

$$u=\frac{\partial\psi}{\partial y}=\left(\frac{bx}{1-\alpha t}\right)f'(\eta), \tag{17}$$

$$v=-\frac{\partial\psi}{\partial x}=-\left(\frac{b\nu}{1-\alpha t}\right)^{\frac{1}{2}}f(\eta). \tag{18}$$

Using equations (15)-(18) in the boundary layer equations, we get the following system of differential equations with the transformed boundary conditions

$$S\left(\frac{\eta}{2}f''+f'\right)+(f')^2-ff''=f'''-K^*\theta^2, \tag{19}$$

$$Pr\left[\frac{S}{2}(\eta\theta'+3\theta)+2f'\theta-f\theta'\right]=\theta'', \tag{20}$$

$$f(0)=0, f'(0)=1, \theta(0)=1, \tag{21}$$

$$f''(\beta)=0, \theta'(\beta)=0, \tag{22}$$

$$f(\beta)=\frac{S\beta}{2} \tag{23}$$

where

$Pr=\frac{\mu C_{vh}}{k}$, the Prandtl number,

$K^*=\frac{\mu_0}{\rho}\left(\frac{K_0}{2\nu}\right)^2 T_{\text{ref}}^2$, the magnetization parameter,

$S=\frac{\alpha}{b}$, the non-dimensional unsteadiness parameter,

$$\beta = \left\{\frac{b}{v(1-\alpha t)}\right\}^{1/2} h, \text{ the dimensionless film thickness.}$$

2.2. Solution procedure.

Similarity transformation (15) is used to reduce the governing equations (9)-(11) to a system of ordinary differential equations (19)-(20). This boundary value problem is converted to an initial value problem and then solved using the shooting technique involving Runge-Kutta-Fehlberg (RKF45) method. The missing values are guessed suitably as given below

$$\begin{gathered}
\frac{dA_1}{d\eta} = A_2, A_1(0) = 0, \\
\frac{dA_2}{d\eta} = A_3, A_2(0) = 1, \\
\frac{dA_3}{d\eta} = S\left(\frac{\eta}{2}A_3 + A_2\right) + A_2^2 - A_1A_3 + K^*A_4^2, A_3(0) = b_1, \\
\frac{dA_4}{d\eta} = A_5, A_4(0) = 1, \\
\frac{dA_5}{d\eta} = Pr\left[\frac{S}{2}(\eta A_5 + 3A_4) + 2A_2A_4 - A_1A_5\right], A_5(0) = b_2.
\end{gathered} \tag{24}$$

The values of the initial slopes b_1 and b_2 are improved using the Newton-Raphson method. The value of the film thickness β is determined based on the condition (23), and the solution corresponding to this particular value of β is noted and analyzed. The numerical solution is obtained with 10^{-6} accuracy.

The present numerical values have been compared with the solutions obtained through the homotopy analysis method by Wang [12] and Noor *et al*. [16] for the limiting case $K^* = 0$ and is as given in table 1. From this table, it is observed that the present values concur well with the previously published values.

Table 1. Comparison of friction coefficient, surface temperature, and wall temperature gradient, when $K^* = 0$.

s	Pr	**Wang [12]**				**Noor *et al*. [16]**				**Present Paper**			
		β	$\frac{f''(0)}{\beta}$	$\theta(1)$	$-\frac{\theta'(0)}{\beta}$	β	$\frac{f''(0)}{\beta}$)	$\theta(1)$	$-\frac{\theta'(0)}{\beta}$	β	$f''(0)$	$\theta(\beta)$	$-\theta'(0)$
0.6		3.13125	−1.19516	-	-	-	-	-	-	3.131711	−1.19513	-	-
	0.01			0.960480	0.042042			0.960480	0.042042			0.960480	0.042042
	0.1			0.692533	0.351377			0.692533	0.351378			0.692533	0.351377
0.8	1	2.15199	−1.2458	0.097884	1.670994	2.15199	−1.245796	0.097881	1.669742	2.151992	−1.24581	0.097884	1.671003
	2			0.024941	2.436878			0.024945	2.428796			0.024863	2.443866
	3			0.008785	3.027163			0.008786	2.965973			0.008312	3.036116
1		1.54362	−1.27776	-	-	1.54362	−1.27763	-	-	1.543616	−1.27777	-	-
	0.01			0.982331	0.033459			0.982331	0.033459			0.982331	0.033459
	0.1			0.843622	0.304963			0.843622	0.304963			0.843622	0.304963
1.2	1	1.12778	−1.27918	0.286717	1.773032	1.12778	−1.27917	0.286712	1.772707	1.12778	−1.27917	0.286717	1.773032
	2			0.128124	2.638325			0.128031	2.638210			0.128123	2.638726
	3			0.067658	3.279744			0.067423	3.275071			0.067645	3.281949
1.4		0.821032	−1.23355	-	-	0.821032	−1.233545	-	-	0.821033	−1.23355	-	-

3. Results and Discussion

The present work analyses ferrofluid's unsteady thin film flow past an unsteady stretching surface and the associated heat transfer characteristics. The similarity transformation has been used to convert the governing PDE's of flow and heat transfer into a system of ODE's which are numerically solved subject to appropriate boundary conditions, using the shooting technique. The influence of magnetization parameter K^*, unsteadiness parameter S, dimensionless film thickness β, and Prandtl number Pr on the dynamics of thin-film flow are investigated. It is observed that the solution exists only for $0 \leq S \leq 2$ (see, Wang [6] and Abel *et al*.[14]). As $S \to 0$ the solution tends to be the exact solution determined by Crane [1] corresponding to $\beta \to \infty$ (infinite film thickness), and the other limiting case $S \to 2$ corresponds to $\beta \to 0$ (infinitesimal film thickness). For the present study, the value of the unsteadiness parameter is chosen between these extreme cases.

Figures 2-3 show the variation of β with the unsteady parameter S for various combinations of Magnetization parameter and Prandtl number. The thickness of the film varies from infinite depth to infinitesimal depth as S varies from 0 to 2. It is also noticed that the increasing values of magnetization parameter K^* Reduces the film thickness. At lower thermal diffusivity (large values of Pr), the diminishing effect of K^* on β is not so prominent.

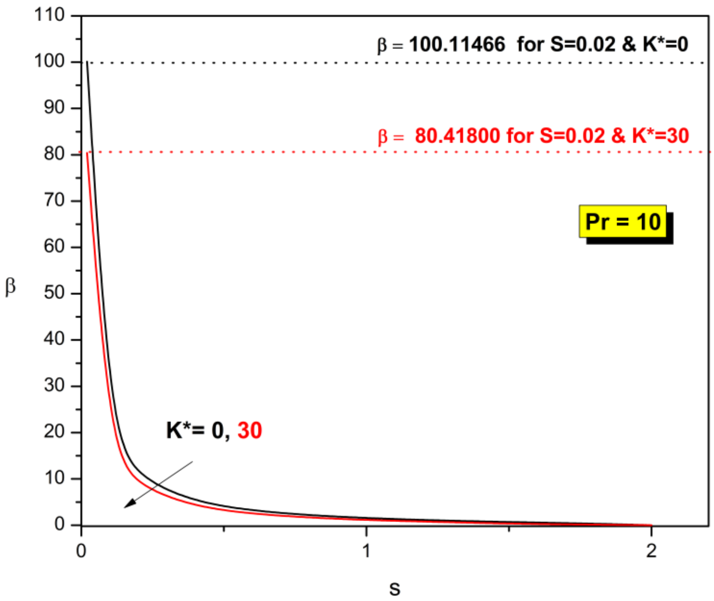

Figure 2. Graph of β versus S when $Pr = 10$.

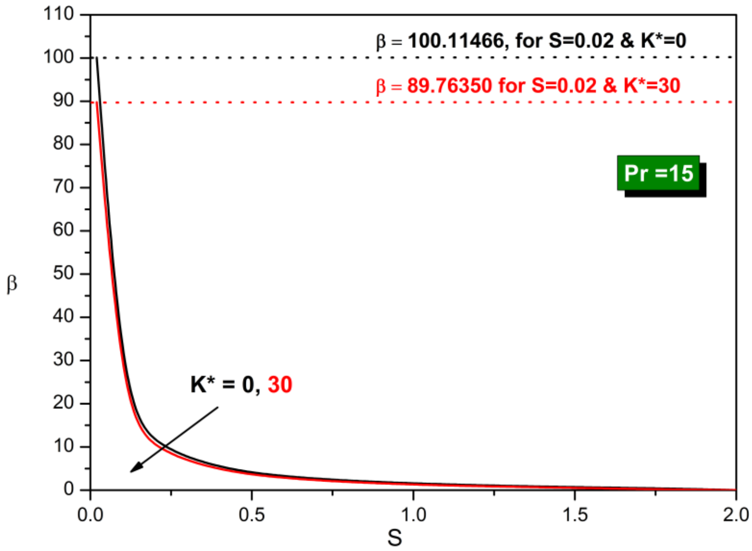

Figure 3. Graph of β versus S when $Pr = 15$.

Figures 4-7 illustrate the influence of K^* on $f'(\eta)$ for various values of unsteady parameter S and Prandtl number Pr. From these graphical representations, it is noticed that K^* has a mixed effect on the velocity profile $f'(\eta)$. Near the free surface $(\eta = \beta)$, increasing values of K^* results in increasing values of $f'(\eta)$, whereas it has an opposite effect in the boundary layer region. The orientation of magnetic moments in the two regions is responsible for this mixed behavior. The viscosity of the carrier fluid directly impacts the velocity profile in the boundary layer region. The Viscosity effects are predominant in the boundary layer region due to the suspended particles of micro/nano size ferrites constituting the ferrofluid. The observed results are qualitatively true in the case of both the chosen values of S and Pr.

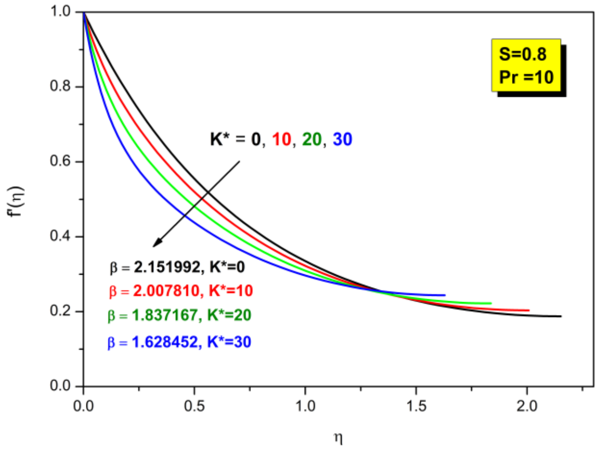

Figure 4. Graph of $f'(\eta)$ when $S = 0.8$ and $Pr = 10$.

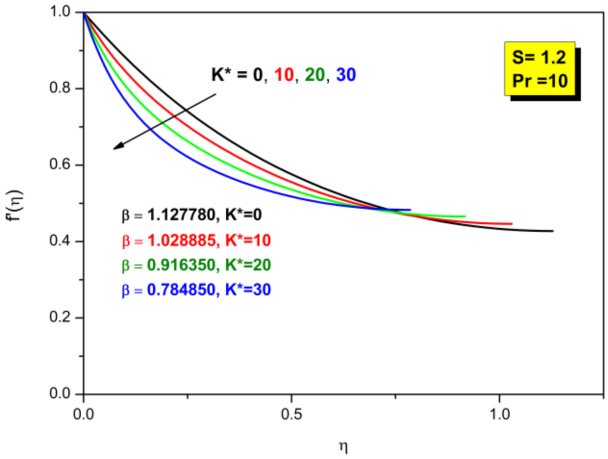

Figure 5. Graph of $f'(\eta)$ when $S = 1.2$ and $Pr = 10$.

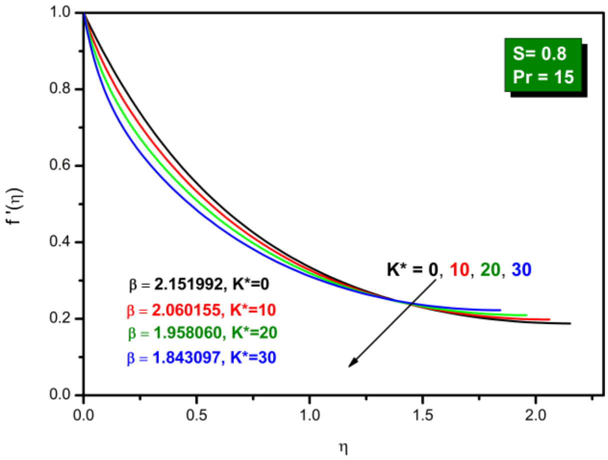

Figure 6. Graph of $f'(\eta)$ when $S = 0.8$ and $Pr = 15$.

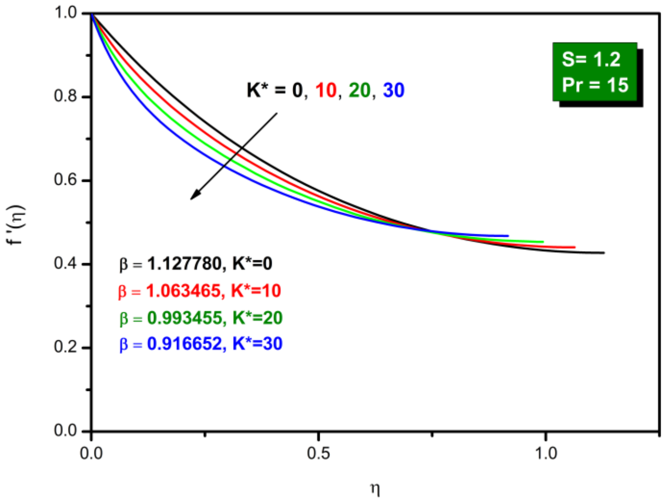

Figure 7. Graph of $f'(\eta)$ when $S = 1.2$ and $Pr = 15$.

Figures 8-11 demonstrate the influence of magnetization parameter K^* on $\theta(\eta)$ for different combinations of S and Pr. From these figures, it is evident that the temperature profile increases significantly with the increase in K^* Values. The magnetic body force, mainly responsible for reducing the velocity in the boundary layer region, will also contribute to the dissipation of heat from frictional heating due to intervention between the liquid layers. This, in turn, increases the temperature in the boundary layer region.

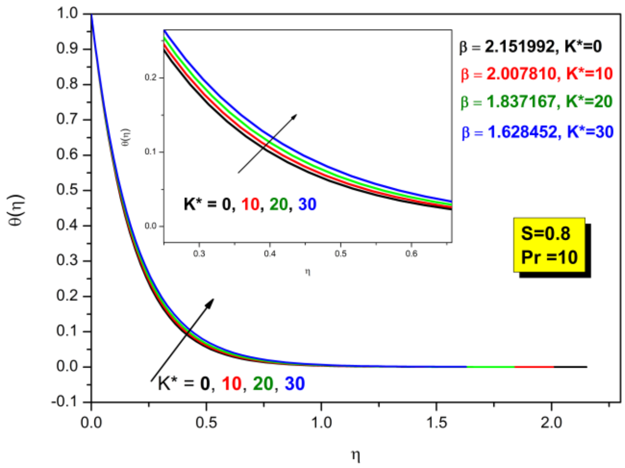

Figure 8. Graph of $\theta(\eta)$ when $S = 0.8$ and $Pr = 10$.

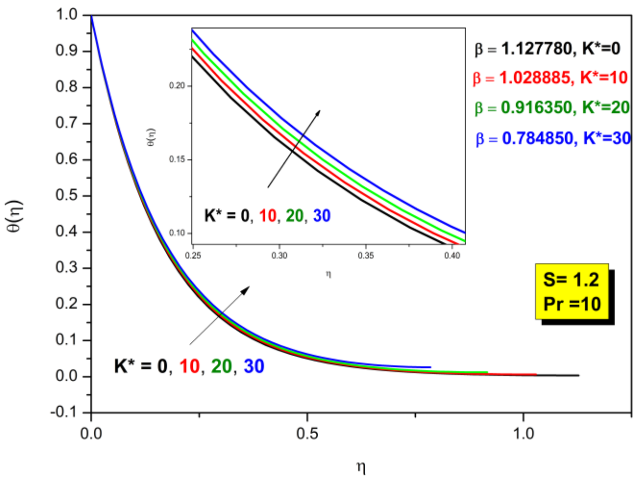

Figure 9. Graph of $\theta(\eta)$ when $S = 1.2$ and $Pr = 10$.

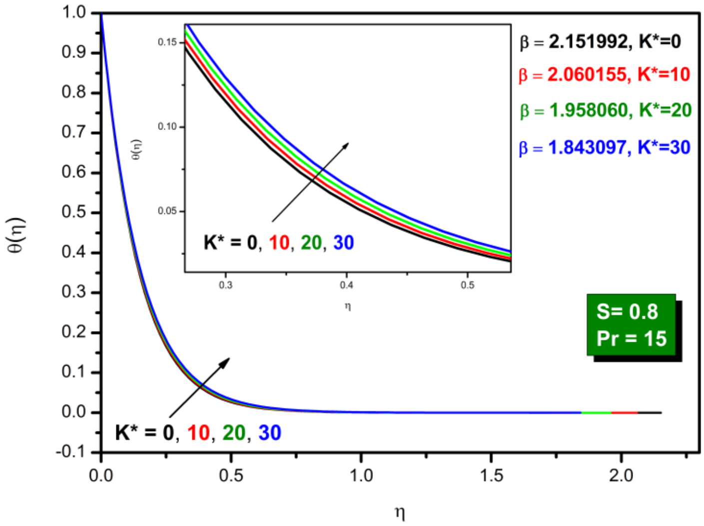

Figure 10. Graph of $\theta(\eta)$ when $S = 0.8$ and $Pr = 15$.

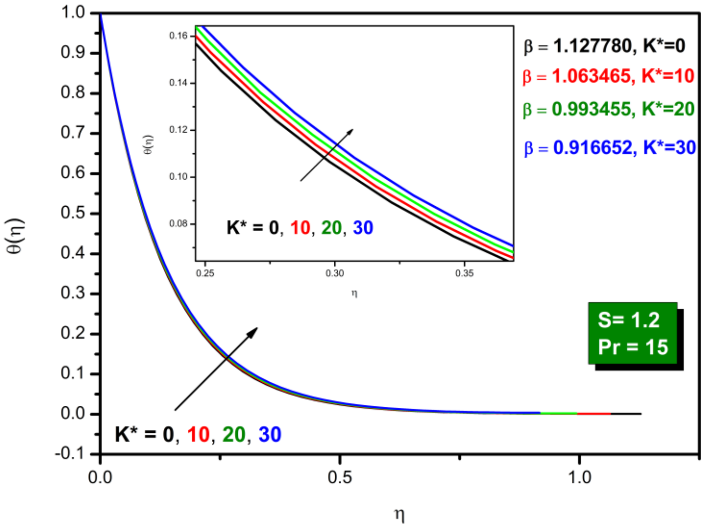

Figure 11. Graph of $\theta(\eta)$ when $S = 1.2$ and $Pr = 15$.

Fig 12 depicts the impact of K^* on the surface velocity $f'(\beta)$ for various combinations of S and Pr. Clearly, $f'(\beta)$ increases with increasing values of K^* for both the chosen values of S and Pr. As mentioned earlier, the orientation of magnetic moments at the surface may be responsible for increasing the surface velocity. Fig 13 illustrates the effect of magnetization parameter K^* on $-f''(0)$ (wall skin friction coefficient) for different combinations of S and Pr. It is observed that $-f''(0)$ increases with an increase in K^* for both the values of S and Pr. It is to be reiterated that the retarding effect of magnetic body force on the motion is responsible for increasing the skin friction at the wall. Fig 14 shows the effect of K^* on $\theta(\beta)$ (surface temperature) for various combinations S and Pr. It is to be noted that $\theta(\beta)$ is an increasing function of K^* for chosen values of S and Pr. The increasing effect is more predominant at higher values of the unsteadiness parameter and lower values of Pr. Fig 15 demonstrates the variation of wall temperature gradient $-\theta'(0)$ with K^* for various values of S and Pr. Clearly, $-\theta'(0)$ is reduced for the two chosen values of S and Pr. The dissipation due to magnetic body force contributes to the increased temperature gradients in the boundary layer by decreasing the wall temperature gradient.

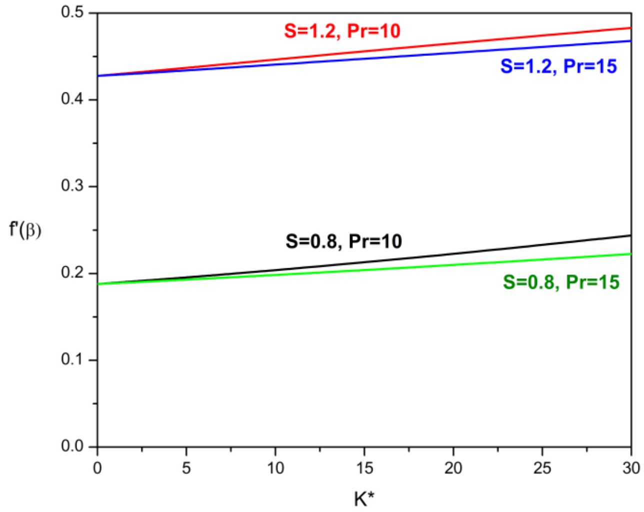

Figure 12. Graph of $f'(\beta)$ with K^*.

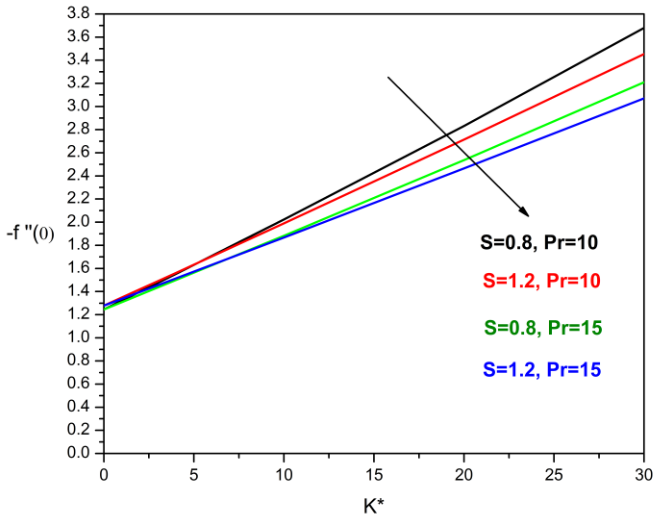

Figure 13. Graph of $-f''(0)$ with K^*.

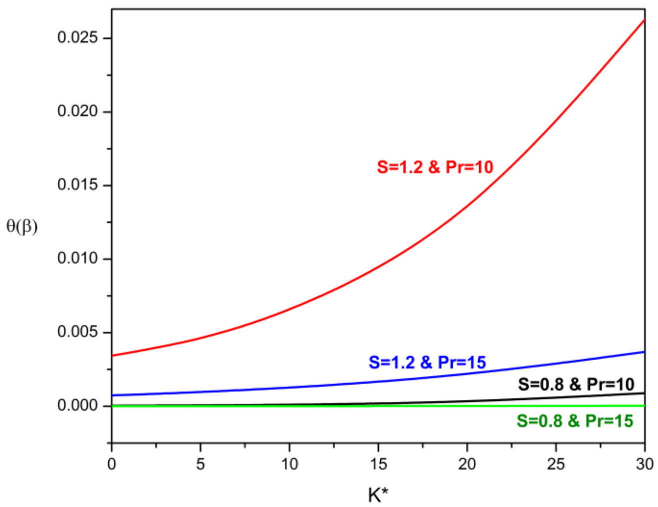

Figure 14. Graph of $\theta(\beta)$ with K^*.

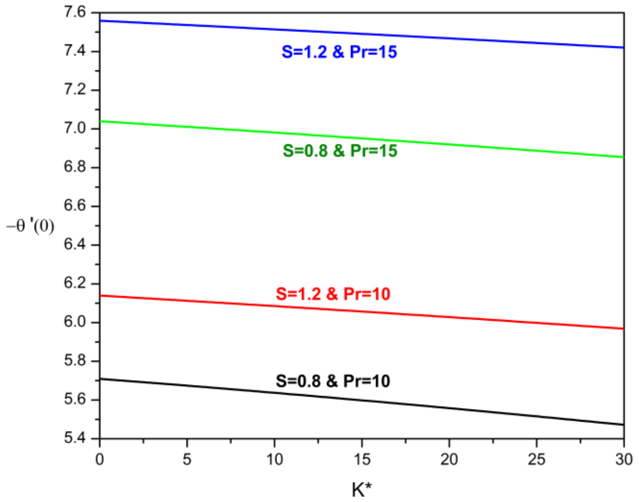

Figure 15. Graph of $-\theta'(0)$ with K^*.

4. Conclusions

The effect of various combinations of unsteadiness parameters, Prandtl number, and magnetization parameters on the flow of ferromagnetic liquid film over a stretching sheet in the presence of an external magnetic field is explored in the present study. The boundary layer equations are transformed into a system of ODE's using the appropriate similarity transformation. The shooting technique is employed to determine the system's numerical solution; ODE's were obtained from the governing equations using similarity transformation. Some of the findings of the present work are listed below.

- Film thickness decays with unsteadiness parameter S, and the magnetization parameter K^*.
- For fixed values of S and K^*Film thickness increases with larger values of Prandtl number.
- K^* has a mixed effect on the velocity profile. Near the free surface, velocity increases with increasing values of K^* & opposite effect is observed near the boundary layer region.
- Skin friction coefficient at the wall increases with the magnetization parameter K^* and the opposite effect is seen in the case of wall heat flux.
- Magnetization parameter K^* has an increasing effect on the temperature field near the free surface. However, temperature decreases for higher values of K^* near the boundary layer region.

Funding

This research received no external funding.

Acknowledgments

B. Azghar Pasha and G. Sowmya are grateful to the research center M S Ramaiah Institute of Technology, Bangalore, India, for their support and encouragement in carrying out their research work. M. Narayana is grateful to The University of the West Indies, Jamaica, for the support. V. Ramachandramurthy is grateful to R. R. Institute of Technology, Bengaluru, India.

Conflicts of Interest

The authors declare no conflict of interest.

References

1. Crane, L.J. Flow past a stretching plate. *Zeitschrift für angewandte Mathematik und Physik ZAMP* **1970**, *2*, 645-647, https://doi.org/10.1007/BF01587695.
2. Andersson, H.I. An exact solution of the Navier-Stokes equations for magnetohydrodynamic flow. *Acta Mechanica* **1995**, *113*, 241-244, https://doi.org/10.1007/BF01212646.
3. Siddheshwar, P.G.; Mahabaleswar, U.S. Effects of radiation and heat source on MHD flow of a viscoelastic liquid and heat transfer over a stretching sheet. *International Journal of Non-Linear Mechanics* **2005**, *40*, 807-820, https://doi.org/10.1016/j.ijnonlinmec.2004.04.006.
4. Abel, M.S.; Mahesha, N. Heat transfer in MHD viscoelastic fluid flow over a stretching sheet with variable thermal conductivity, non-uniform heat source and radiation. *Applied Mathematical Modelling* **2008**, *32*, 1965-1983, https://doi.org/10.1016/j.apm.2007.06.038.
5. Mahabaleshwar, U.S.; Sarris, I.E.; Hill, A.A.; Lorenzini, G.; Pop, I. An MHD couple stress fluid due to a perforated sheet undergoing linear stretching with heat transfer. *International Journal of Heat and Mass Transfer* **2017**, *105*, 157-167, https://doi.org/10.1016/j.ijheatmasstransfer.2016.09.040.
6. Wang, C.Y. Liquid film on an unsteady stretching surface. *Quarterly of applied Mathematics* **1990**, *48*, 601-610, https://doi.org/10.1090/qam/1079908.
7. Andersson, H.I.; Aarseth, J.B.; Braud, N.; Dandapat, B.S. Flow of a power-law fluid film on an unsteady stretching surface. *Journal of Non-Newtonian Fluid Mechanics* **1996**, *62*, 1-8, https://doi.org/10.1016/0377-0257(95)01392-X.
8. Andersson, H.I.; Aarseth, J.B.; Dandapat, B.S. Heat transfer in a liquid film on an unsteady stretching surface. *International Journal of Heat and Mass Transfer* **2000**, *43*, 69-74, https://doi.org/10.1016/S0017-9310(99)00123-4.
9. Dandapat, B.S.; Santra, B.; Andersson, H.I. Thermocapillarity in a liquid film on an unsteady stretching surface. *International Journal of Heat and Mass Transfer* **2003**, *46*, 3009-3015, https://doi.org/10.1016/S0017-9310(03)00078-4.
10. Dandapat, B.S.; Maity, S. Flow of a thin liquid film on an unsteady stretching sheet. *Physics of fluids* **2006**, *18*, https://doi.org/10.1063/1.2360256.
11. Dandapat, B.S.; Maity, S.; Kitamura, A. Liquid film flow due to an unsteady stretching sheet. *International Journal of Non-Linear Mechanics* **2008**, *43*, 880-886, https://doi.org/10.1016/j.ijnonlinmec.2008.06.003.
12. Wang, C. Analytic solutions for a liquid film on an unsteady stretching surface. *Heat and Mass Transfer* **2006**, *42*, 759-766, https://doi.org/10.1007/s00231-005-0027-0.
13. Chen, C.H. Effect of viscous dissipation on heat transfer in a non-Newtonian liquid film over an unsteady stretching sheet. *Journal of Non-Newtonian Fluid Mechanics* **2006**, *135*, 128-135, https://doi.org/10.1016/j.jnnfm.2006.01.009.
14. Abel, M.S.; Mahesha, N.; Tawade, J. Heat transfer in a liquid film over an unsteady stretching surface with viscous dissipation in presence of external magnetic field. *Applied Mathematical Modelling* **2009**, *33*, 3430-3441, https://doi.org/10.1016/j.apm.2008.11.021.
15. Santra, B.; Dandapat, B.S. Unsteady thin-film flow over a heated stretching sheet. *International Journal of Heat and Mass Transfer* **2009**, *52*, 1965-1970, https://doi.org/10.1016/j.ijheatmasstransfer.2008.09.036.
16. Noor, N.F.; Abdulaziz, O.; Hashim, I. MHD flow and heat transfer in a thin liquid film on an unsteady stretching sheet by the homotopy analysis method. *International Journal for Numerical Methods in Fluids* **2010,** *63*, 357-73, https://doi.org/10.1002/fld.2078.
17. Dandapat, B.S.; Singh, S.K. Thin film flow over a heated nonlinear stretching sheet in presence of uniform transverse magnetic field. *International Communications in Heat and Mass Transfer* **2011**, *38*, 324-328, https://doi.org/10.1016/j.icheatmasstransfer.2010.11.009.
18. Maity, S. Thermocapillary flow of thin liquid film over a porous stretching sheet in presence of suction/injection. *International Journal of Heat and Mass Transfer* **2014**, *70*, 819-826, https://doi.org/10.1016/j.ijheatmasstransfer.2013.11.070.
19. Dandapat, B.S.; Singh, S.K.; Maity, S. Thin film flow of bi-viscosity liquid over an unsteady stretching sheet: an analytical solution. *International Journal of Mechanical Sciences* **2017**, *130*, 367-374, https://doi.org/10.1016/j.ijmecsci.2017.06.027.
20. Dandapat, B.S.; Maity, S.; Singh, S.K. Thin double-layer film development over a flat stretching sheet. *Zeitschrift für angewandte Mathematik und Physik* **2018**, *69*, 1-19, https://doi.org/10.1007/s00033-018-1003-0.
21. Krishanan, R.; Maity, S.; Dandapat, B.S. Unsteady Flow Of Casson Liquid Film On A Stretching Sheet With Radiative Heat Transfer. *Surface Review and Letters* **2020**, *27*, https://doi.org/10.1016/j.molliq.2016.07.145.

22. Khan, M.I.; Alzahrani, F. Entropy-optimized dissipative flow of Carreau–Yasuda fluid with radiative heat flux and chemical reaction. *The European Physical Journal Plus* **2020** *135*, 1-6, https://doi.org/10.1140/epjp/s13360-020-00532-3.
23. Farooq, U.; Ijaz, M.A.; Khan, M.I.; Isa, S.S.; Lu, D.C. Modeling and non-similar analysis for Darcy-Forchheimer-Brinkman model of Casson fluid in a porous media. *International Communications in Heat and Mass Transfer* **2020** *119*, https://doi.org/10.1016/j.icheatmasstransfer.2020.104955.
24. Chu, Y.M.; Rehman, M.I.; Khan, M.I.; Nadeem, S.; Kadry, S.; Abdelmalek, Z.; Abbas, N. Transportation of heat and mass transport in hydromagnetic stagnation point flow of Carreau nanomaterial: Dual simulations through Runge-Kutta Fehlberg technique. *International Communications in Heat and Mass Transfer* **2020** *118*, https://doi.org/10.1016/j.icheatmasstransfer.2020.104858.
25. Aldabesh, A.; Khan, S.U.; Habib, D.; Waqas, H.; Tlili, I.; Khan, M.I.; Khan, W.A. Unsteady transient slip flow of Williamson nanofluid containing gyrotactic microorganism and activation energy. *Alexandria Engineering Journal* **2020,** *59*, 4315-4328, https://doi.org/10.1016/j.aej.2020.07.036.
26. Li, Y.X.; Khan, M.I.; Gowda, R.P.; Ali, A.; Farooq, S.; Chu, Y.M.; Khan, S.U. Dynamics of aluminum oxide and copper hybrid nanofluid in nonlinear mixed Marangoni convective flow with entropy generation: Applications to renewable energy. *Chinese Journal of Physics* **2021** *73*, 275-287, https://doi.org/10.1016/j.cjph.2021.06.004.
27. Nayak, M.K.; Shaw, S.; Khan, M.I.; Makinde, O.D.; Chu, Y.M.; Khan, S.U. Interfacial layer and shape effects of modified Hamilton's Crosser model in entropy optimized Darcy-Forchheimer flow. *Alexandria Engineering Journal* **2021** *60*, 4067-4083, https://doi.org/10.1016/j.aej.2021.02.010.
28. Song, Y.Q.; Khan, S.A.; Imran, M.; Waqas, H.; Khan, S.U.; Khan, M.I.; Qayyum, S.; Chu, Y.M. Applications of modified Darcy law and nonlinear thermal radiation in bioconvection flow of micropolar nanofluid over an off centered rotating disk. *Alexandria Engineering Journal* **2021** *60*, 4607-4618, https://doi.org/10.1016/j.aej.2021.03.053.
29. Varun Kumar, R.S.; Alhadhrami, A.; Punith Gowda, R.J.; Naveen Kumar, R.; Prasannakumara, B.C. Exploration of Arrhenius activation energy on hybrid nanofluid flow over a curved stretchable surface. *ZAMM-Journal of Applied Mathematics and Mechanics* **2021,** *101*, https://doi.org/10.1002/zamm.202100035.
30. Berrehal, H.; Sowmya, G.; Makinde, O.D. Shape effect of nanoparticles on MHD nanofluid flow over a stretching sheet in the presence of heat source/sink with entropy generation. *International Journal of Numerical Methods for Heat & Fluid Flow* **2021,** *32*, 1643-1663, https://doi.org/10.1108/HFF-03-2021-0225.
31. Saleh, B.; Madhukesh, J.K.; Varun Kumar, R.S.; Afzal, A.; Abdelrhman, Y.; Aly, A.A.; Punith Gowda, R.J. Aspects of magnetic dipole and heat source/sink on the Maxwell hybrid nanofluid flow over a stretching sheet. *Proceedings of the Institution of Mechanical Engineers, Part E: Journal of Process Mechanical Engineering* **2022**, https://doi.org/10.1177/09544089211056243.
32. Madhukesh, J.K.; Alam, M.M.; Varun Kumar, R.S.; Arasaiah, A.; Ahmad, I.; Gorji, M.R.; Prasannakumara, B.C. Exploring magnetic dipole impact on Maxwell hybrid nanofluid flow over a stretching sheet. *Proceedings of the Institution of Mechanical Engineers, Part E: Journal of Process Mechanical Engineering* **2022,** https://doi.org/10.1177/09544089211073267.
33. Saleh, B.; Madhukesh, J.K.; Varun Kumar, R.S.; Afzal, A.; Abdelrhman, Y.; Aly, A.A.; Punith Gowda, R.J. Aspects of magnetic dipole and heat source/sink on the Maxwell hybrid nanofluid flow over a stretching sheet. *Proceedings of the Institution of Mechanical Engineers, Part E: Journal of Process Mechanical Engineering* **2022,** https://doi.org/10.1177/09544089211056243.
34. Varun Kumar, R.S.; Gunderi Dhananjaya, P.; Naveen Kumar, R.; Punith Gowda, R.J.; Prasannakumara, B.C. Modeling and theoretical investigation on Casson nanofluid flow over a curved stretching surface with the influence of magnetic field and chemical reaction. *International Journal for Computational Methods in Engineering Science and Mechanics* **2022,** *23*, 12-19, https://doi.org/10.1080/15502287.2021.1900451.
35. Rosensweig, R.E. *Ferrohydrodynamics.* Cambridge University Press, 1st edition, New York. **1985**.
36. Andersson, H.I.; Valnes, O.A. Flow of a heated ferrofluid over a stretching sheet in the presence of a magnetic dipole. *Acta Mechanica* **1998**, *128*, 39-47, https://doi.org/10.1007/BF01463158
37. Abel, M.S.; Siddheshwar, P.G.; Mahesha, N. Numerical solution of the momentum and heat transfer equations for a hydromagnetic flow due to a stretching sheet of a non-uniform property micropolar liquid. *Applied Mathematics and computation* **2011**, *217*, 5895-5909, https://doi.org/10.1016/j.amc.2010.12.081.
38. Narayana, M.; Rani Titus, L.S.; Abraham, A.; Sibanda, P. Modelling micropolar ferromagnetic fluid flow due to stretching of an elastic sheet. *Afrika Matematika* **2004**, *25*, 667-679, https://doi.org/10.1007/s13370-013-0145-7.
39. Majeed, A.; Zeeshan, A.; Ellahi, R. Unsteady ferromagnetic liquid flow and heat transfer analysis over a stretching sheet with the effect of dipole and prescribed heat flux. *Journal of Molecular liquids* **2016**, *223*, 528-533, https://doi.org/10.1016/j.molliq.2016.07.145.
40. Ramana Reddy, J.V.; Sugunamma, V.; Sandeep, N. Effect of frictional heating on radiative ferrofluid flow over a slendering stretching sheet with aligned magnetic field. *The European physical journal plus* **2017**, *132*, 1-13, https://doi.org/10.1140/epjp/i2017-11287-1.

41. Jalili, B.; Sadighi, S.; Jalili, P.; Ganji, D.D. Characteristics of ferrofluid flow over a stretching sheet with suction and injection. *Case Studies in Thermal Engineering* **2019**, *14*, https://doi.org/10.1016/j.csite.2019.100470.
42. Bhandari, A.; Husain, A. Optimization of heat transfer properties on ferrofluid flow over a stretching sheet in the presence of static magnetic field. *Journal of Thermal Analysis and Calorimetry* **2021**, *144*, 1253-1270, https://doi.org/10.1007/s10973-020-09636-5.
43. Sivaraj, C.; Gubin, V.E.; Matveev, A.S.; Sheremet, M.A. Impacts of uniform magnetic field and internal heated vertical plate on ferrofluid free convection and entropy generation in a square chamber. *Entropy* **2021**, *23*, https://doi.org/10.3390/e23060709.
44. Ali, B.; Siddique, I.; Khan, I.; Masood, B.; Hussain, S. Magnetic dipole and thermal radiation effects on hybrid base micropolar CNTs flow over a stretching sheet: Finite element method approach. *Results in Physics* **2021**, *25*, https://doi.org/10.1016/j.rinp.2021.104145.
45. Mohamed, M.K.A.; Yasin, S.H.M.; Salleh, M.Z.; Alkasasbeh, H.T. MHD stagnation point flow and heat transfer over a stretching sheet in a blood-based casson ferrofluid with newtonian heating. *Journal of Advanced Research in Fluid Mechanics and Thermal Sciences* **2021,** *82*, 1-11, https://doi.org/10.37934/arfmts.82.1.111.
46. Gangadhar, K.; Sobhana Babu, P.R.; Venkata Subba Rao, M. Microstructure and inertial characteristic of a magnetite Ferro fluid over a stretched sheet embedded in a porous medium with viscous dissipation using the spectral quasi-linearisation method. *International Journal of Ambient Energy* **2021,** *42*, 769-778, https://doi.org/10.1080/01430750.2018.1563823.
47. Tahir, W.; Althobaiti, N.; Kousar, N.; Alhazmi, S.E.; Bilal, S.; Riaz, A. Effects of Homogeneous-Heterogeneous Reactions on Maxwell Ferrofluid in the Presence of Magnetic Dipole along a Stretching Surface: A Numerical Approach. *Mathematical Problems in Engineering* **2022**, *2022*, https://doi.org/10.1155/2022/4148401.
48. Azghar Pasha, B.; Narayana, M.; Sowmya, G.; Ramachandramurthy, V. Numerical investigation of ferromagnetic liquid film flow over an unsteady stretching surface in the presence of radiation and aligned magnetic field. *Heat Transfer* **2022**, *51*, https://doi.org/10.1002/htj.22499.